Journal of Digital Convergence
Vol. 16. No. 2, pp. 19-26, 2018

ISSN 1738-1916
https://doi.org/10.14400/JDC.2018.16.2.019

Improved Lung and Pulmonary Vessels Segmentation and Numerical Algorithms of Necrosis Cell Ratio in Lung CT Image

Joon-Ho Cho[1], Sung-Ryong Moon[2*]
[1]Department of Electronics Convergence Engineering, Wonkwang University
[2]Department of Electronic Engineering, Wonkwang University

흉부 CT 영상에서 개선된 폐 및 폐혈관 분할과 괴사 세포 비율의 수치적 알고리즘

조준호[1], 문성룡[2*]
[1]원광대학교 전자융합공학과, [2]원광대학교 전자공학과

Abstract We proposed a numerical calculation of the proportion of necrotic cells in pulmonary segmentation, pulmonary vessel segmentation lung disease site for diagnosis of lung disease from chest CT images. The first step is to separate the lungs and bronchi by applying a three-dimensional labeling technique from a chest CT image and a three-dimensional region growing method. The second step is to divide the pulmonary vessels by applying the rate of change using the first order polynomial regression, perform noise reduction, and divide the final pulmonary vessels. The third step is to find a disease prediction factor in a two-step image and calculate the proportion of necrotic cells.

Key Words : Lung, Necrosis Cell, Region Growing Method, Rolling Ball Algorithm, Vessel

요 약 흉부 CT 영상에서 폐 질환의 진단을 위해서 폐 분할, 폐혈관 분할과 폐 질환 부위에 대한 괴사 세포 비율의 수치적 계산을 제안 하였다. 첫 번째 단계는 흉부 CT 영상에서 3차원 레이블링 기법과 3차원 영역 성장법을 적용하여 폐와 기관지를 분리한다. 두 번째 단계는 폐혈관 분할은 1차 다항식 회귀(Polynomial Regression)를 사용한 변화율을 적용하여 분할한 다음, 잡음 제거를 실시하여 최종의 폐혈관을 분할한다. 세 번째 단계는 2단계 이미지 에서 질환 예상 인자를 발견하고, 괴사 세포의 비율을 계산하는 것이다. 질환 예상인자는 폐에 대해서 3차원 레이블링 기법을 적용하였고, 각 레이블 중심 값을 관측하여 변화가 없는 레이블을 찾는다. 이렇게 찾은 질환 예상 인자는 조영제 투입 전/후 영상을 정합한 뒤, 면적을 비교하면 폐의 괴사 세포 비율을 계산할 수 있다.

주제어 : 괴사 세포, 롤링볼 알고리즘, 영역 성장법, 폐, 폐혈관

1. Introduction

The computer-assisted diagnosis that uses the image analysis and subdividing of X-ray Computed Tomography (CT) has been used in medical diagnosis and treatment.

High-resolution multi-detector computed tomography (CT) plays an important role in the treatment and diagnosis of lung cancer. At the same time, it helps doctors improve the diagnostic ability but also increase the burden of reading slices. In order to solve this problem, computer aided detected system is provided. And lung region segmentation is the first step of the automatic system. At present, the existing traditional

*This paper was supported by Wonkwnag University in 2016
*Corresponding Author : Sung-Ryong Moon(srmoon@wku.ac.kr)
Received December 4, 2017 Revised January 10, 2018
Accepted February 20, 2018 Published February 28, 2018

segmentation methods are mostly based on significant difference between lung regions and the peripheral tissue. This kind of method is suitable for the segmentation without pathological region. But lists eight cases of pathological lung which cannot get the correct results based on traditional methods [1-3]. However, in recent years, the studies, especially contain big tumor located in arbitrary position, about pathological lung segmentation have just begun. For Juxta-pleura nodules, fit the Bezier curved surface by affine transformation to the target lung and then improve the result by the active contour algorithm[4-7]. When the lesion appears at the top of the lung or at the bottom of the lung, the method produces the segmentation errors. Surface model is established by marching cube algorithm, then identify and remove the problematic area, last repair and fit surface by radia basis function(RBF)[8]. This method is suitable for filling small lesions area, such as Juxta-vascular nodule. This method is not suitable for the lung. This method is suitable for lung area which is including local sharp feature and large area pathology. For lung which is including large pathology, It provide an interstitial lung disease segmentation method based on texture feature[9,10]. This method is a kind of pixel-based classification method and is suitable for the pathology area whose texture is large difference with normal area. When pathology area is connected with pulmonary mediastinal region, this method cannot get correct result. Segment pathological lung based on atlas registration[11-16], it can get high accuracy rate. This method also can handle lung which is including all kinds of pathological changes, but the processing time is beyond tolerance in clinic.

In this paper, segment pathological lung which include large tumor based on improved rolling ball algorithm. And we expressed numerically necrosis cell ratio of abnormal regions into CAD system. This paper was composed of Chapter 2 that describes for the segmentation of the lung, vessels and numerically necrosis cell ratio of abnormal regions, and Chapter 3 that contains the simulation and consideration using Matlab software, and Chapter 4 that contains the Conclusions.

2. Proposed Algorithm

The starting of the lung and airway segmentation are started from removing in detail the surround structure after leaving only the chest image in chest CT images.

First step is to obtain only the chest area that other structure is removed from the chest CT. The optimal threshold and the three-dimensional region growing method were applied on the entire chest CT image. The second step is the segmentation of the pulmonary vessels. The applied method for this step is that the threshold value is obtained by using the polynomial regression analysis of the histogram change rate from the lung image, and the pulmonary vessels containing the noise are segmented by this threshold value. And, the images of the pulmonary vessels that the remaining noise is removed by the three-dimensional connected component labeling method of the diaphragm and the binary image using the three-dimensional region growing method were obtained. The third step is the segmentation of the lung. In this step, the abnormal of pulmonary outsides was identified by applying the separation of left/right lungs through the open operation, and the improved rolling ball algorithm. And if the abnormal exists, that area was removed, and the pulmonary outsides were connected with newly second-order polynomial. As a result, the part removed in the first step because the lung disease was included in the pulmonary breastwork was restored.

Expected factor of lung disease and an arithmetical calculation of necrosis cell ratio in abnormal regions have obtained make a comparison between before and after injected with Contrast.

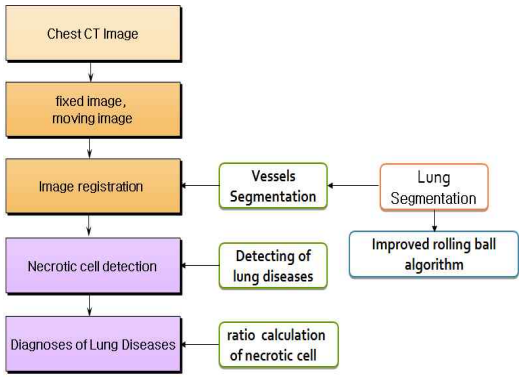

Fig. 1. Proposed Algorithm

2.1 Lung Segmentation

Otsu algorithm is one of many methods used for the image segmentation. In this paper, this algorithm was firstly applied to the segmentation of the lung and airway area in the chest area according to the brightness value in the chest CT. However, if you apply this method, the noise from other organs in the body and the chairs, etc will be included. So, the post-processing is required, and in this paper, three-dimensional region growing method through three-dimensional labeling was applied. Fig. 2 is the three-dimensional image applying Otsu algorithm. Noise is included as shown in Fig. 2.

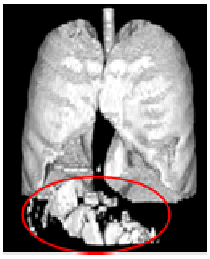

Fig. 2. Existing lung and Airway Segmentation

Three-dimensional region growing method through three-dimensional labeling is progressed in the following order: First, the labeling is performed on all the parts connected to the three-dimension. And, the inspector must fine the label that has the largest area. Where, the labels that have the largest area are the lungs and the airway. Finally, a random seed point is selected, and three-dimensional region growing method is applied on it. As a result, only the lung and airway area will be remained, and all the noise are removed. Fig. 3 shows the image of the lungs and airway that the noise is removed, and it can be checked that the noise contained in Fig. 1 was removed.

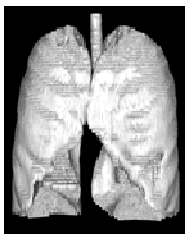

Fig. 3. Proposed lung Segmentation

2.2 Pulmonary Vessels Segmentation

In order to determine the threshold of the pulmonary vessels segmentation, the authors analyzed the histogram using entire lungs image. And the data that became the obstructive element in the determination of threshold, and the brightness value was zero (0) by occupying large part in the image was excluded in the histogram analysis. The brightness values of the histogram written in Figure used the brightness value (unit 16 value) of CT image, and the change rate of histogram was analyzed based on the lung image which is the final image of Fig. 4 If whole lung image is represented in the histogram and the change rate of histogram was analyzed, the results represents as the numerical values over thousands or tens of thousands. The change rate value of these large numbers is not suitable for using as data that calculate the threshold of the pulmonary vessels. In the case of the histogram normalized dividing the frequency of voxels that represents other type of histogram by the total frequency, because the frequency of voxels exceed millions, the normalized value appears too small numerical value, and also the change rate appears too small, so these data is not suitable to calculate the threshold value.

In this paper, the rate of the histogram was normalized so that the rate of change of the histogram has the suitable numerical value to calculate the

threshold. In other words, the brightness value (horizontal axis) of the histogram and the range (vertical axis) of voxel frequency were normalized to the same size, and the results are the same as shown in Fig. 4.

In order to investigate the rate of change of the rate-normalized histogram, if calculating the rate of change using the slope of first-order polynomial at the sequent two point, the results are the same as shown in Fig. 5 The flow of the rate of change as shown in Fig. 5 is the result difficult to use as data for calculating the threshold. In order to solve the heavy fluctuation of the rate of change and effectively calculate the threshold, in this paper, the slope of the first-order polynomial regression applying the least square method to the rate-normalized histogram in Fig. 4 was used as the rate of change. The number of sample data to obtain the first-order polynomial regression was 30, and the results are same as shown in [Fig. 4] The results in Fig. 4 can be non-logically seen the flow of the rate of change, and can be easily applied in the calculation of threshold.

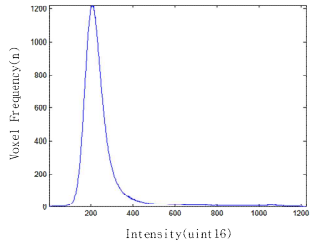

Fig. 4. Rate-Normalized Histogram

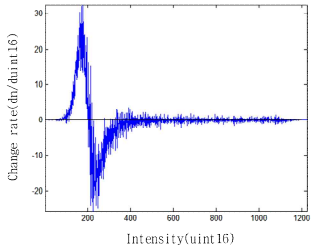

Fig. 5. Rate of Change of Rate-Normalized Histogram

The optimal Thresholding is used as the threshold for image segmentation in most cases. However, because the distribution of the average brightness value of pulmonary vessels is lower than the optimal threshold, the distribution should be controlled to lower value than the optimal threshold in order to calculate the effective threshold. In this paper, the rate of change of first-order polynomial regression in Fig. 6 was analyzed in order to calculate the effective threshold, and the brightness value at the position with the rate of change of -1 was experimentally used as the threshold of the pulmonary vessels segmentation.

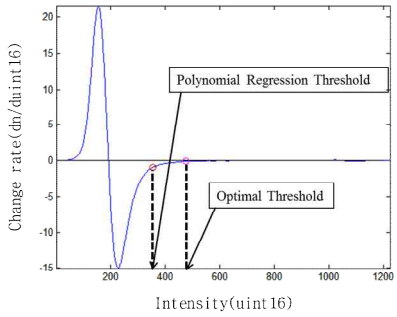

Fig. 6. Rate of Change using First-order Polynomial Regression

2.3 Pulmonary Vessels Purification

If the pulmonary vessels are segmented using the brightness-based tresholding, because the diaphragm or noise that has similar brightness value as the pulmonary vessels can be divided together, the purification process is required in order obtain the accurate pulmonary image. In this paper, in order to purify the pulmonary vessels, the diaphragm was extracted by using three-dimensional region growing method, and the pulmonary vessels purification method was used by using the three-dimensional connected component labeling method of a binary image.

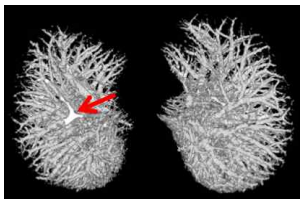

Fig. 7. Diaphragm difficult to remove by Circularity

In this paper, the method that selects the seed point of the left and right diaphragms by the eccentricity and the size of the connection elements, and extracts the diaphragm image by determining the left side and right side diaphragm area by using the three-dimensional region growing method at the seed point, was proposed.

2.4 Arithmetical calculation of necrosis cell ratio in abnormal regions

Expected factor of lung disease be able to detect use of the level value information obtained through the lung Vessels. The proposed method is to find continuously unchanged level value in the range obtained lung vessel leveling.

The error range of expected factor is set up a two slice in lung CT, To study was performed under limited conditions to be found in at least three sheets of image slices.

If such conditions are found expected factor in the Lung disease, After injected with Contrast, the same way search lung disease and the registration of the two lung CT images.

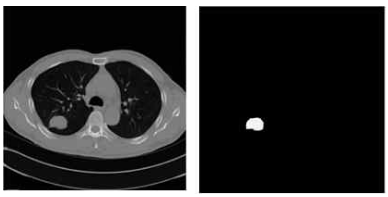

(a) Fixed image (Before contrast injection)

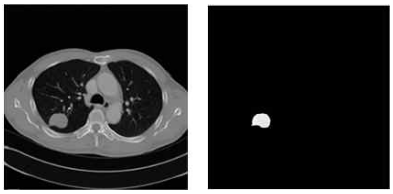

(b) Moving image (After contrast injection)

Fig. 8. Images before and after contrast injection

The ratio of necrosis cell was calculated by the difference between the two images when more than 50 is recognized as a necrosis.

(a) Registered image (b)necrosis cell image

Fig. 9. The ratio of necrosis cell image

3. Simulation and Consideration

The sequence of simulation is same as follows: In step 1, the lung and the airway are divided in the chest CT. The optimal threshold and the three-dimensional region growing method by the three-dimensional labeling described in Section 3 were applied. In step 2, the separation of airway was performed by separating into before and after the carina. Fig. 10 shows the separation of the lung and the airway in step 1, and the result of the airway separation in two type of chest CT.

(a)Lung Segmentation (b)Airway Segmentation

Fig. 10. Lung and Airway Segmentation in Chest CT

This method was that the left/right lungs were segmented, and the outside of the lungs for abnormal was checked by applying transformed rolling ball algorithm, and if abnormal was found, that part was removed, and it was restored to the normal lungs by connecting the outside of the lung in the form of second-order polynomial.

Step 3 is the segmentation of the lungs. The proposed method in this paper was that the left/right lungs were separated, and the outside of the lungs for abnormal was checked by applying transformed rolling ball algorithm, and if abnormal was found, that part was removed, and it was restored to the normal lungs by connecting the outside of the lung in the form of

second-order polynomial.

Fig. 11 shows the segmentation of pulmonary vessels. Fig. 11-(a) shows the image that the threshold is set up by the optimal threshold method and the pulmonary vessels are segmented, and Fig. 11-(b) is the resulting image that the pulmonary vessels are segmented by the threshold obtained analyzing the rate of change of first-order polynomial regression. It can be seen that more pulmonary vessels can be segmented by the proposed method in this paper.

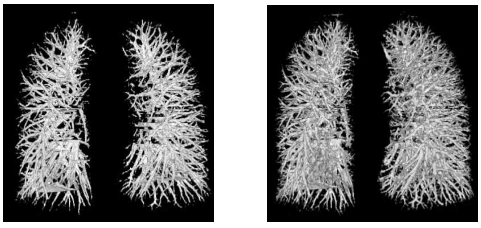

(a) (b)

(a) Use of Optimal Threshold
(b) Use of Threshold analyzing by Polynomial Regression

Fig. 11. Result of pulmonary vessels segmentation using histogram analysis.

In Fig. 12, the noise that is difficult to see as the pulmonary vessels exists, and the noise was removed using the proposed method

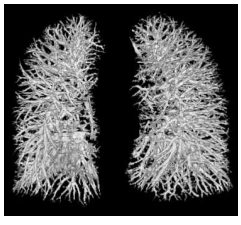

Fig. 12. Pulmonary vessels image after removing the noise

Fig. 13 shows the expected factor in pulmonary disease. it was detected after pulmonary vessels algorithm.

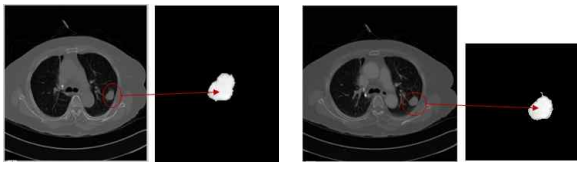

(a) fixed image (b) moving image

Fig. 13. Expected factor in pulmonary disease

In order to calculate the percentage of necrotic cells should be applied only matched by portion of Fig. 14 In contrast we consider only the between before and after the correspond. Definition of the ratio of necrotic cells was calculated by comparing the images before and after contrast injection. In this paper, it was defined as fifty or less.

Fig. 14 is a calculation process of necrotic cells.

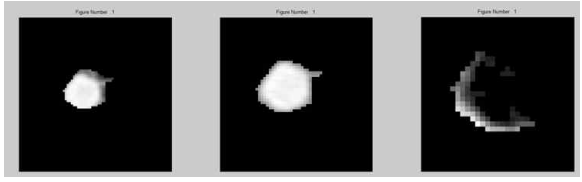

(a) (b) ©

(a) Image of before contrast injection
(b) Image of after contrast injection
(c) Image of alive cell

Fig. 14. Ratio calculation process of cell necrosis

Table 1. Ratio of necrotic cells

	Ratio of necrotic cells(%)	Ratio of alive cells(%)
1	57	43
2	68	32
3	50.4	49.6
4	97.8	2.2
5	64.1	35.9
6	62.9	37.1
7	75.7	24.3
8	80.4	19.6
⋮	⋮	⋮
99	42.2	57.8
100	70.6	29.4
101	85.5	14.5
102	84.5	15.5
103	70.6	29.4
104	46.2	53.8
mean	65.60385	34.39423

Table 1 is a table showing the Ratio of necrotic cells.

4. CONCLUSION

In this paper, segment pathological lung which include large tumor based on improved rolling ball

algorithm. And we expressed numerically necrosis cell ratio of abnormal regions into CAD system. The lung segmentation were obtained by the region growing method through the optimal threshold and three-dimensional labeling. As a result, the images of the lung and airway that the noise is removed from the chest CT could be obtained. The segmentation of pulmonary blood vessels, initial pulmonary vessels were segmented by obtaining the threshold using the polynomial regression analysis of the rate of change in the histogram on the lung image, and then the final pulmonary vessels image is obtained by removing the diaphragm and the noise. In order to calculate the percentage of necrotic cells should be applied only matched by portion of Fig. 14. In contrast we consider only the between before and after the correspond. Definition of the ratio of necrotic cells was calculated by comparing the images before and after contrast injection. Thus, this proposed method can also be utilized in the diagnosis and treatment system developing the imaging biomarkers for the lung disease patients by the automatic segmentation of the lungs, pulmonary vessels. and Ratio calculation of necrotic cells.

REFERENCES

[1] X1. Meng, Y. Qiang, S. Zhu, C. Fuhrman , JM. Siegfried & J. Pu.(2012). Illustration of the obstacles in computerized lung segmentation using examples. *Med Phys, 39(8),* 498-491.
DOI: 10.1118/1.4737023

[2] M. S. Brown, M. F. McNitt-Gray, N. J. Mankovich, J. G. Goldin, J. Hiller, L. S. Wilson & D. R. Aberle.(1997). Method for segmenting chest CT image data using an anatomic model: Preliminary results. *IEEE Trans. Medical Imaging. 16(6).* 828-839.
DOI: 10.1109/42.650879

[3] S. Hu, E. A. Hoffman & J. M. Reinhardt.(2001). Accurate Lung Segmentation for Accurate Quantitation of Volumetric X-Ray CT Images. *IEEE Transactions on Medical Imaging. 20(6).* 490-498.
DOI: 10.1109/42.929615

[4] T. Kitasaka, K. Mori, J. Hasegawa & J. Toriwaki. (2003). Lung area extraction from 3-D chest X-ray CT images using a shape model generated bya variable Bezier surface. *Syst. Comput. Jpn.. 34(4),* 60-71.
DOI: 10.1002/scj.1201

[5] Y.Y.Yim, H. L. Hong & Y. G. Shin. (2005). Automatic Lung Segmentation using Hybrid Approach. *Journal of KIISE : Software and Applications. 32(7),* 625-635.
DOI: 10.1118/1.3147146

[6] D. Bartz, D. Mayer, J. Fischer & S. Ley.(2003). Hybrid Segmentation and Exploration of the Human Lungs. *Proc. of IEEE Visualization, 14(3),* 177-184.
DOI:10.1109/VISUAL.2003.1250370

[7] Y. Masutani, H. MacMahon & K. Doi.(2002). Computerized Detection of Pulmonary Embolism in Spiral CT Angiography Based on Volumetric Image Analysis. *IEEE Transactions on Medical Imaging. 21(12),* 1517-1523.
DOI: 10.1109/TMI.2002.806586

[8] J. Pu, D. S. Paik, X. Meng, J. E. Roos & G. D. Rubin.(2011). Shape break and-repair strategy and its application to automated medical image segmentation. *IEEE Transactions on Visualization and Computer Graphics. 17(1),* 115-124.
DOI: 10.1109/TVCG.2010.56

[9] A. Jemal, T. Murray, E. Ward, A. Samuels, R. C. Tiwari, A. Ghafoor, E.J. Feuer & M. J. Thun. (2005). Cancer statistics 2005. *A Cancer Journal for Clinicians. 55(1),* 10 - 30.
DOI: 10.3322/canjclin.55.1.10

[10] J. Wang, Q. Li & F. Li.(2009). Automated segmentation of lungs with severe interstitial lung disease in CT. *Med. Phys. 36(10),* 4592-4599.
DOI: 10.1118/1.3222872

[11] I. Sluimer, M Prokop. & B. van Ginneken. (2005). Toward automated segmentation of the pathological lung in CT. *IEEE Trans. Med. Imag. 24(8),* 1025-1038.
DOI: 10.1109/TMI.2005.851757

[12] Y. H. Shi, F. H. Qi, Z. Xue, L. Y. Chen, K. K Ito, H. Matsuo & D. Shen.(2008). Segmenting lung fields in serial chest radiographs using both population-based and patient-specific shape statistics. *IEEE trans. Med. Imag. 27(4),* 481-494.
DOI: 10.1109/TMI.2007.908130

[13] A. A. Farag & J. H. Graham. (2013). A novel approach for lung nodules segmentation in chest CT using Levelsets. *IEEE Trans image processing. 22(2),* 5202-5213.

DOI: 10.1109/TIP.2013.2282899

[14] M. Rogers & J. Graham.(2002). Robust active shape model search. *Proceedings of the European Conference on Computer Vision. 1(1),* 517-530.
DOI : https://doi.org/10.1007/3-540-47979-1_35

[15] M. J. Shin & D. Y. Kim.(2012). Pulmonary vascular Segmentation and Refinement On the CT Scans. *The Journal of the Korean Institute of Information and Communication Engineering. 16(3),* 591-597.
DOI : 10.6109/jkiice.2012.16.3.591

[16] S. H. Lee et al.(2014). A Study on the Usefulness of 3D Imaging in Micro-CT for Observing the Microstructure of Mice. *Journal of Digital Convergence. 12(3),* 367-375.
DOI: 10.14400/JDC.2014.12.3.367

조 준 호(Cho, Joon Ho) [정회원]

- 2002년 2월 : 원광대학교 대학원 제어계측공학과(공학석사)
- 2007년 2월 : 원광대학교 대학원 제어계측공학과(공학박사)
- 2007년 4월 ~ 현재 : 원광대학교 전자융합공학과 조교수

- 관심분야 : 전기전자, 로봇비전, 의료영상처리
- E-Mail : cho1024@wku.ac.kr

문 성 룡(Moon, Sung Ryong) [정회원]

- 1982년 2월 : 전북대학교 대학원 전자공학과(공학석사)
- 1986년 2월 : 전북대학교 대학원 전자공학과(공학박사)
- 2005년 4월 ~ 현재 : 원광대학교 전자공학과 교수

- 관심분야 : 신경망 및 퍼지, 디지털시스템제어, 영상처리
- E-Mail : srmoon@wku.ac.kr